Earthquake scenario-specific framework for spatial accessibility analysis (SAA) of emergency shelters: a case study in Xichang City, Sichuan Province, China

Ziyue Wang[1,2], Jia Cheng[3]* and Chong Xu[1,2]

[1]National Institute of Natural Hazards, Ministry of Emergency Management of China, Beijing, China, [2]Key Laboratory of Compound and Chained Natural Hazards Dynamics, Ministry of Emergency Management of China, Beijing, China, [3]School of Earth Sciences and Resources, China University of Geosciences (Beijing), Beijing, China

The spatial accessibility of emergency shelters, indicating the difficulty of evacuation and rescue, is crucial for disaster mitigation and emergency management. To analyze accessibility, an effective approach is to evaluate the service capacity of emergency shelters. Multifaceted factors were employed to enhance the quantitative accuracy of accessibility indicators. However, scenario-specific analysis has not been emphasized. Considering the devastating potential of great earthquake disasters, we cannot ignore the impact of these scenarios on emergency shelter accessibility, especially in areas with high seismic risk. In this study, we developed an earthquake scenario-specific framework for spatial accessibility analysis (SAA), which integrates the service capacity of emergency shelters and the impact of strong ground motion and fault rupturing. We applied this framework to the urban area of Xichang City in Sichuan Province, western China. Xichang City, located in the linked area of the Anninghe fault and Zemuhe fault with many extreme historical earthquake disaster records, is prone to high seismic risk. We firstly collected emergency shelter and road network data in Xichang City. We then applied SAA based on the road network, using the network analysis method. After that, we analyzed the impact of strong ground motion on accessibility and generated the setback zone of fault rupturing. We integrated the effect of strong ground motion on accessibility within the setback zone of active faults. Finally, we generated a comprehensive accessibility map, considering both the predicted strong ground motion and potential fault rupturing. Our results show that the accessibility level changed in several towns of urban Xichang City due to strong ground motion and fault rupturing. The accessibility level decreased in Lizhou, Xingsheng, and Anning Towns. For areas with mapped fault lines, the accessibility level is Very-Low. Our results demonstrate the impact of earthquake damage on the accessibility of emergency shelters and the complexity of evacuation in earthquake scenarios. In general, we added earthquake rupturing

and ground motion characteristics into the SAA framework. This framework will help us enhance the reliability of SAA and the feasibility of seismic vulnerability evaluation.

1 Introduction

Earthquake disasters rank as the most destructive natural disasters in the world (Albulescu, 2023). With the rapid development of urbanization, the growing exposure of populations and structures aggravates the seismic risk in urban areas (Zou et al., 2023). Such unpromising circumstances necessitate the optimization of earthquake disaster mitigation. The foundation of an optimal formulation lies in knowledge about the location, capacity, and spatial accessibility of critical emergency facilities (Albulescu, 2023). Emergency shelters are one of the most essential emergency facilities, providing temporary resettlement, medical services, and emergency command centers for residents. The spatial accessibility of emergency shelters depends on the complexity of evacuation in an emergency and reflects the effectiveness of mitigation strategies and emergency management. The SAA of emergency shelters can also assist in formulating strategies to optimize disaster mitigation for high seismic risk areas.

Once an earthquake occurs, taking shelter is the very first instinct of residents, which demands mobility and accessibility (Zou et al., 2023). Exploring the spatial distribution of emergency shelters is an effective approach for identifying their accessibility to refugees (Gall, 2004; Chang and Liao, 2015). A map of spatial accessibility distribution could visualize the ease of reaching emergency shelters and evaluate the rationality of their allocation.

The methods used for the SAA of urban facilities mainly encompass typical spatial analysis methods such as buffer analysis (Zhang, 2020) and network analysis (Hou and Jiang, 2014; Albulescu, 2023; Yan, 2023). Methods are constantly developing, with advanced methods combined with GIS technology. The gravity model, which considers the relationship between supply- and demand-sides, can be an essential companion to GIS spatial analysis technology to distinguish the radiation coverage of different-sized areas (Zhang, 2020). As a special form of the gravity model, the two-step floating catchment area (2SFCA) method can assist in the study of urban emergency facilities. For example, the Gaussian two-step mobile search method, which is an improved 2SFCA method, introduces a Gaussian function with an excellent fit for distance decay. This function can help obtain a more accurate accessibility indicator (Tong et al., 2021; Jiang et al., 2023). In addition, a 2SFCA method with a variable service radius and evacuation radius was proposed to deal with the differences in emergency shelter service capacities and population distribution (Su, Chen, and Cheng, 2022a). Moreover, typical map applications (e.g., Google Map and Baidu Map) also stimulate accessibility evaluation. For instance, the application programming interface (API) can provide automatic time cost calculations for real-time travel (Wang et al., 2019) and navigation data (Shen et al., 2020). As the accuracy of the accessibility index constantly improves, the quantitative assessment of spatial accessibility continues to evolve.

However, qualitative analysis involving particular scenarios has not been much emphasized, although multiple scenarios can affect the accessibility of emergency shelters. For example, demographic density, evacuation capacity across age groups, population spatial temporal distribution, and even topographic factors can lead to differences in evacuation time (Su, Chen, and Zhang, 2022b; Zou et al., 2023). Moreover, the accessibility of emergency shelters in disaster scenarios is of great concern (Zhang and Yun, 2019). The accessibility might be undermined at different levels due to severe damage. Earthquake damage can be distinguished into direct damage (e.g., shaking or failure of over-bridges and roads) and indirect damage (e.g., street blockages due to debris from collapsed buildings) (Anastassiadis and Argyroudis, 2007). Strong ground motion and fault rupturing can cause catastrophic damage to buildings and road surfaces. During the 2008 M8 Wenchuan earthquake, the buildings along the fault-ruptured area were all significantly destroyed because of sudden fault rupturing (Xu et al., 2009). Moreover, open space damage caused by shaking and collapsed buildings can indirectly impede evacuation and rescue in the immediate aftermath (Francini et al., 2020; Bernardini and Ferreira, 2022). Dramatic destruction due to fault rupturing and strong ground motion can significantly impede emergency evacuations. In such situations, accessibility to emergency shelters would be impaired. To better assist in emergency management, we must explore the reasonable SAA of emergency shelters for earthquake scenarios.

In this study, we developed an earthquake scenario-specific framework for SAA. This framework integrated the service capacity of urban facilities with the characteristics of earthquake scenarios. Except for the spatial distribution of emergency shelters, we were able to gain an insight into the fault rupturing and strong ground motion caused by earthquake disasters. First, we operated the spatial service area of emergency shelters through network analysis. Based on the service area distribution, we generated the impact of strong ground motion and fault rupturing on the level of accessibility. Finally, we generated a comprehensive distribution map of the level of accessibility to emergency shelters in earthquake scenarios.

We employed this framework in the urban area of Xichang City in western China. After analyzing the impact of strong ground motion and fault rupturing characteristics, we determined the changes in the accessibility level in several towns of Xichang City. We also identified the practical service area of emergency shelters in earthquake scenarios. Our results are reasonable as we considered the potential effects caused by earthquake disaster characteristics.

In the subsequent sections, we introduce the historical earthquake records and the extent of the study area in Section 2. Then, in Section 3, we illustrate the framework combined with the case study in Xichang City. We display the results in Section 4

FIGURE 1
Geological location of Xichang City.
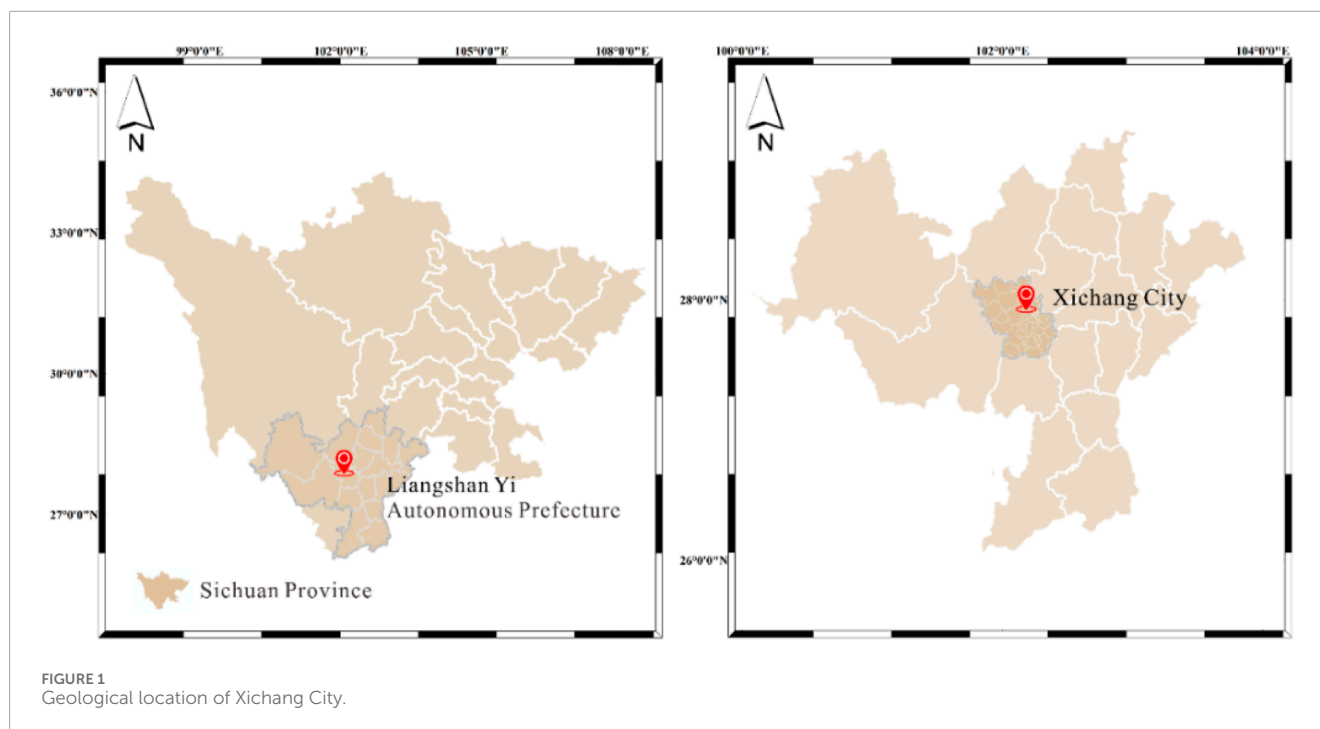
and discuss them in Section 5. The last section draws conclusions for this study.

2 Study area

Xichang City, located in southwestern Sichuan Province, China, is the capital of the Liangshan Yi Autonomous Prefecture (Figure 1). Xichang City's population has increased from 700,000 to 966,000 in the past 10 years. Infrastructure construction there has expanded ~ four times, with an urbanization rate of 68.48% (http://www.xichang.gov.cn/zfxxgk/zfxxgknr/tjsj_31356/202305/t20230526_2487868.html, last accessed in January 2024). The increased population and expanded inhabited structures can raise issues of natural disaster prevention, especially in high seismic risk zones. To cope with emergency evacuation issues in earthquake-prone areas, the construction of a reasonable SAA framework for emergency shelters is particularly important.

Xichang City is in an area with frequent earthquake occurrences. Due to the collision between the Indian and Eurasian plates, the eastern Tibetan plateau exhibits active crustal extrusion at a rate of approximately 10 mm/yr, resulting in frequent historical earthquakes. This pattern is particularly evident on large-scale boundary faults such as the Xianshuihe fault, the Anninghe fault, the Zemuhe fault and the Xiaojiang fault. Xichang City is located at the link of the Anninghe fault and the Zemuhe fault (Figure 2), both with high left-lateral strike–slip rates of ~6.5 mm/yr (Ren et al., 1990; Xu et al., 2003; Shen et al., 2005; Cheng et al., 2012).

Historically, Xichang City has suffered significantly from devastating earthquakes—the 814 M7 earthquake, the 1489 M6.8 earthquake, the 1536 M7.5 earthquake, the 1732 M6.8 earthquake, and the 1850 M7.8 earthquake

(Ren et al., 1993; Wen, 2000; Jia Cheng et al., 2021; Jia Cheng, 2023). These historical earthquakes and their damage (Liu, 1989; Zhang et al., 1998; Min et al., 2005) are illustrated in Supplementary Table S1.

In the 1489 M6.8 earthquake, Xichang City was near the assumed VIII or VIII+ intensity zone. The seismic intensity for cities situated about 100 km from Xichang (e.g., Mianning and Yuexi) also reached VIII or VIII+. Cities located approximately 600 km–700 km from Xichang (e.g., Suining, Yingshan, and Lingshui) are near the IV-intensity zone (Supplementary Figure S1). In the 1536 M7.5 earthquake, Xichang City was in the IX intensity zone. Cities situated approximately 400 km from Xichang (e.g., Dayi, Chengdu, Chongqing, and Ziyang) were near the assumed VI or VI+ intensity zone (Supplementary Figure S2A). In the 1732 M6.8 earthquake, Xichang City was in the IX intensity zone (Supplementary Figure S2B). In the 1850 M7.8 earthquake, Xichang City was in the region where seismic intensity is assumed to be X (Supplementary Figure S2C).

Xichang City is still in a high-risk zone for earthquakes. Recent studies have proposed a sizable seismic gap in the Anninghe–Zemuhe–Daliangshan region, both from the lengthy intervals between historical earthquakes and the scarcity of M_L2.5 earthquakes since 1980 (Yi et al., 2004; Wen et al., 2008; Yi, Wen, and Su, 2008). The expansion of the population and the number of high buildings make the evacuation of residents difficult in large earthquake events. Hence, we applied our SAA methodology to emergency shelters in Xichang City.

Prompt evacuation and rescue are crucial for preventing fatalities and severe injuries in residential buildings in an emergency (Chen et al., 2023). Increasingly large populations in urban areas also increase exposure to natural disasters. This situation should be emphasized in disaster mitigation research (Huang et al., 2019;
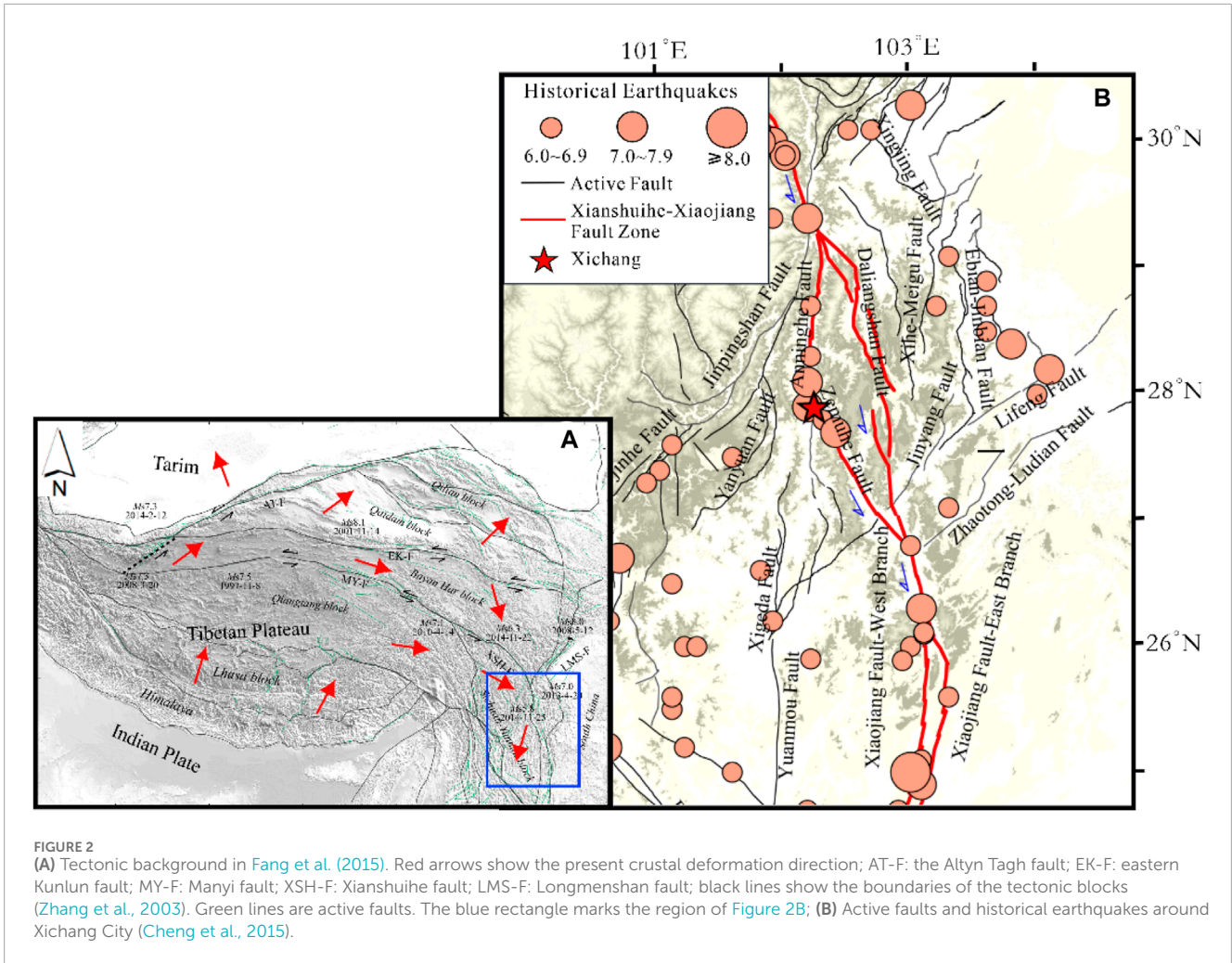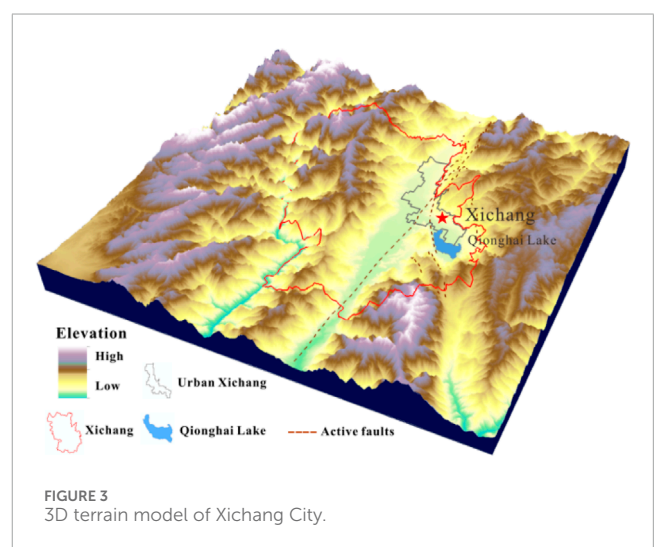
FIGURE 2
(A) Tectonic background in Fang et al. (2015). Red arrows show the present crustal deformation direction; AT-F: the Altyn Tagh fault; EK-F: eastern Kunlun fault; MY-F: Manyi fault; XSH-F: Xianshuihe fault; LMS-F: Longmenshan fault; black lines show the boundaries of the tectonic blocks (Zhang et al., 2003). Green lines are active faults. The blue rectangle marks the region of Figure 2B; **(B)** Active faults and historical earthquakes around Xichang City (Cheng et al., 2015).

Elliott, 2020; Iglesias et al., 2021; Albulescu, 2023). In this case, we employed SAA on emergency shelters in urban Xichang City, which is in a high seismic risk area. Using its population density data and remote sensing images, we extracted an area with an obviously high population density in Xichang City. Here, we analyzed raster data from Grid Population of the World Version 4 (GPW v4) in 2020 (https://sedac.ciesin. Columbia. edu/data/collection/gpw_ v4, last accessed November 2023) and divided them into different categories according to the attribute values of each raster. Finally, we clipped out the areas with significant population density as the study area (Figure 3).

3 Methodology

Here, we develop an earthquake scenario-specific SAA framework for cities with high seismic risks, such as Xichang City. Based on quantitative analysis with the network analysis method, we focus on the characteristics of earthquake scenarios (e.g., strong ground motion and fault rupturing). The procedure in this framework contains three main steps. First, we analyzed the accessibility of emergency shelters based on road network data using network analysis. Next, we assessed the impact of

FIGURE 3
3D terrain model of Xichang City.

strong ground motion on accessibility. Finally, we calculated the impact of fault rupturing on accessibility and generated a comprehensive accessibility distribution map. We illustrate the workflow in Figure 4.

FIGURE 4
Workflow of the earthquake scenario-specific framework for SAA.
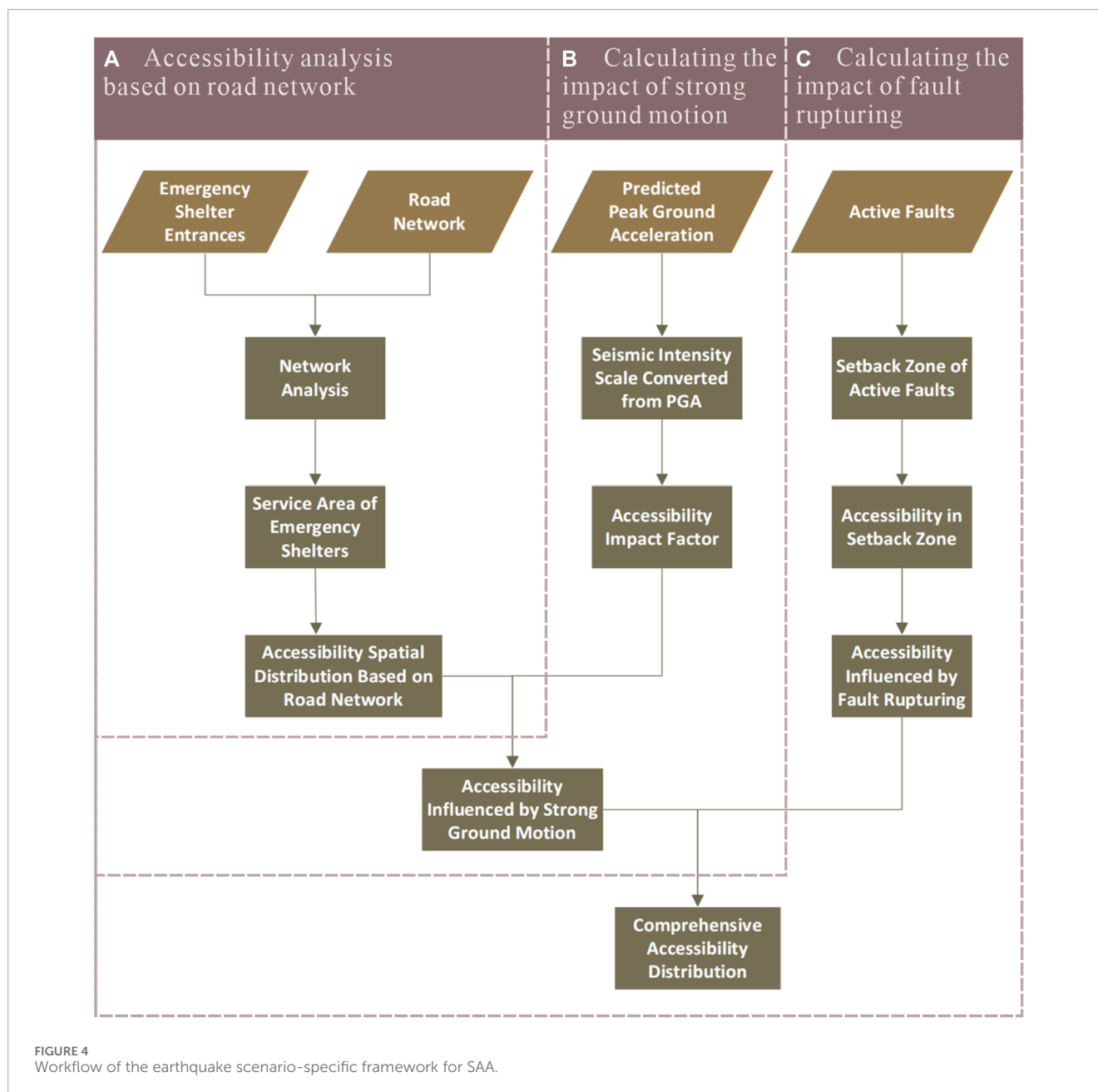
3.1 Data

In this study, datasets for analysis included emergency shelters, the urban road network, predicted peak ground motion, and the active faults. We illustrate the detailed information and source of these data in Table 1.

Urban emergency shelters refer to sites with certain functional facilities which can protect people from direct or indirect damage in disasters and provide essential life support after disasters (Qian, 2010). The local government makes some improvements and modifications to extend emergency evacuation functions on public open spaces (e.g., parks and squares). In the event of a disaster, these improved facilities can supply temporary resettlement and fundamental medical services for injuries (Li et al., 2023).

Evacuation efficiency relies on the reasonability of emergency shelter spatial distribution. Here, we applied SAA to emergency shelters in Xichang City to analyze the reasonability of their distribution.

We used remote sensing images from Google Earth Pro to select proper sites as emergency shelters. In urban areas with congregations of tall buildings, a qualified emergency shelter requires the following conditions: flat terrain, open areas, and no tall buildings around to ensure safety (Amini Hosseini, Asadzadeh Tarebari, and Mirhakimi, 2022). According to these conditions, we selected some spacious and flat sites, such as playgrounds, parks, squares, sizeable open-air parking lots, and stadiums (Figures 5A–E). Among the selected sites, we found some large open spaces covered with green dust cloth on remote sensing images (Figure 5F), which may be alternate building

TABLE 1 Data source and details.

Dataset	Source	Details and processing
Emergency shelters	Manual selection	Reference for selection: GB 21734-2008 (General Administration of Quality Supervision, Inspection and Quarantine of the People's Republic of China, 2008), GB/T 33744-2017 (General Administration of Quality Supervision, Inspection and Quarantine of the People's Republic of China, 2017), and GB/T 35624-2017 (General Administration of Quality Supervision, Inspection and Quarantine of the People's Republic of China, 2017). General principles: i. Being flat and spacious; ii. Away from high buildings and structures.
Urban road network	Open Street Map	Extraction via Open Street Map. Manual pre-procession via QGIS.
Predicted Peak Ground Acceleration (PGA)	475-year PGA values (Jia Cheng et al., 2021)	Calculation of PGA values using a compatible fault model from geological slip rates and geodetic slip rates inverted in an elastic block model
Active faults	Updated and integrated active faults dataset (Wu et al., 2023)	Update and integration of the dataset based on the most recent 20-year region-scale active fault survey data (1:250,000–1:50,000), including geophysical probing, drill logging, offset landform measuring, and sample dating, as well as geometric and kinematic parameters of exposed and blind faults, paleo-earthquake sequences, and recurrence intervals

sites. Although they meet the basic requirements of being flat with no tall buildings around, we still excluded these sites due to the possibility of construction in the short term.

Since every second in an earthquake emergency evacuation is essential for minimizing casualties (Chen et al., 2023), we identified accurate locations of selected emergency shelters for subsequent calculations. Most emergency shelters are sizeable and open while people's running speed is limited, so we directly labeled the location of entrances instead of the emergency shelter center in our SAA. Residents from different directions can reach the shelters from shorter distances through multiple entrances. Our approach used the time to the entrances of available emergency shelters other than the time to the center. This procedure makes our results more reasonable.

We employed Open Street Map (OSM) data for the urban road network data and preprocessed them through QGIS. After extracting and clipping the road network vector data for the urban areas of Xichang, we simplified the road network to ensure the efficiency and rationality of subsequent analysis. We removed the line elements unsuitable for emergency evacuation from the attribute table, such as track, rail, river, stream, administrative, and

boundary. Moreover, we determined the anomalies in the road network vector data, such as unreasonable dangles, pseudo-nodes, and self-intersections. Dangles are not allowed in the road network topology, except for dead ends (Liu et al., 2017). The pseudo-nodes indicate that the complete lines are separated into discrete segments by the unconnected nodes (Qin, 2010). We also examined them using the error inspector and corrected them to ensure the implementation of subsequent network analysis.

We used active fault data from the updated and integrated database of Wu et al. (2023). In their database, region-scale active fault survey data (1:250,000–1:50,000) for the past 20 years are used to update and integrate the active fault data in the Seismotectonic Map of China and its Adjacent Regions (1:4,000,000).

We used predicted PGA to represent strong ground motion. The 475-year PGA results are from Jia Cheng et al. (2021). Two sets of the results were supplied in their work: a compatible fault model from geological slip rates and geodetic slip rates inverted in an elastic block model. Their results are reasonable, as they considered both the fault slip rate and multi-segment rupture events in their PGA results.

3.2 Spatial accessibility analysis based on the road network

In this process, we operated the SAA via the Network Analysis Tool. Network analysis allows for the optimal investigation of network structure and resources by analyzing the network state. This method can also simulate the resource flow and distribution of the network (Liu et al., 2017). The positioning and allocation of resources in the network system is one of the main application scenarios of network analysis (Qin, 2010). The generation of a service area includes the components of a road network located within a specified impedance. The service area distribution of facilities can represent the accessibility of urban facilities for residents in different locations without a specific travel direction. Therefore, network analysis is an effective method for facility SAA.

We used the following steps for SAA based on the road network. First, we calculated the time cost and added it to the attribute table of road network vector data. Next, we established a new network dataset. We set the impedance to the value of the Time Cost field and did not assign a specific direction of travel. We chose these selected emergency shelters as the facilities in our dataset. Then, we started to generate the service area based on road network data. We created a new service area in the network analysis tool and loaded the emergency shelter entrances into the facility point layer. In analysis settings, we input the break value of impedance. Here, we set the break value at 5-min intervals for the former and 15-min intervals for the last two (0–5 min, 5–10 min, 10–15 min, 15–30 min, and ≥30 min). Finally, we chose to merge by break value in multiple facilities options and set rings as overlay types.

After all the setup work, we obtained the time cost distribution circles as the accessibility to emergency shelters. Time cost indicates the complexity of evacuation routes, so we set the accessibility level based on different time circles (Table 2). Five accessibility levels were used in our results: Very-High, High, Medium, Low, and Very-Low.
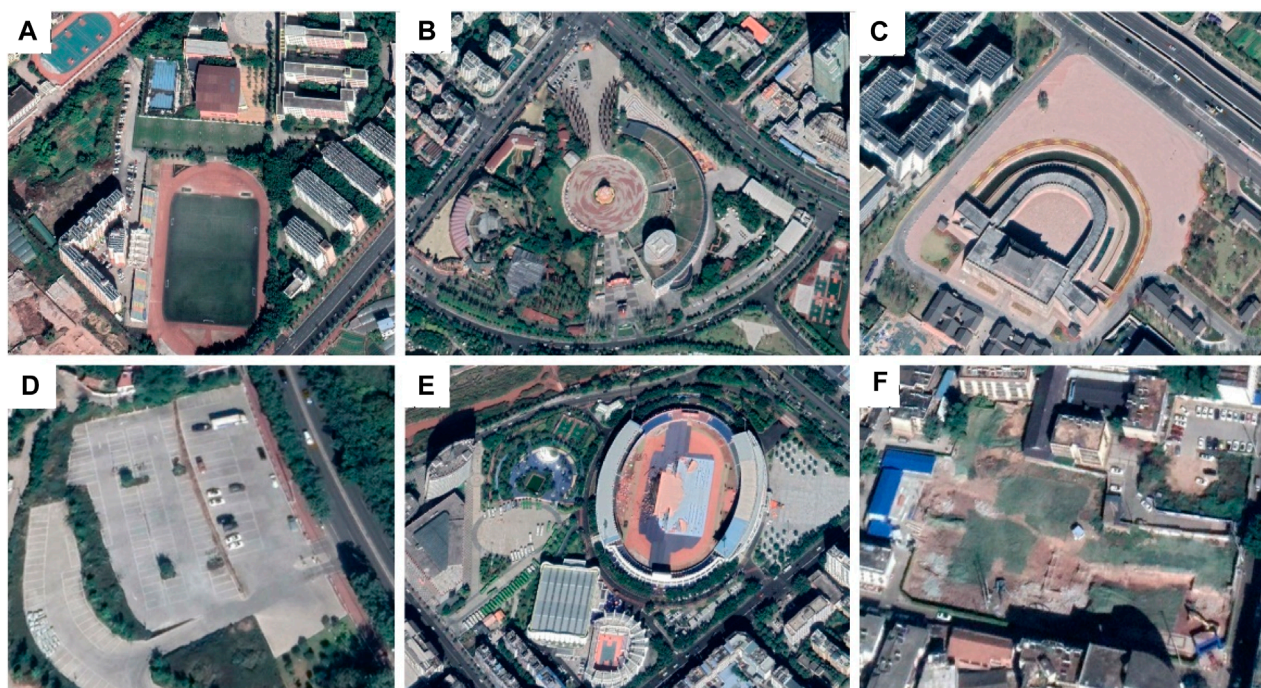
FIGURE 5
Examples of selected emergency shelters and excluded sites: **(A)** playground; **(B)** park; **(C)** square; **(D)** sizeable open-air parking lots; **(E)** open-air stadium; **(F)** space covered with green dust cloth which might be used for future engineering and construction.

TABLE 2 Relationship between time cost for evacuation and corresponding accessibility level.

Time cost for evacuation (min)	Accessibility level
≤5	Very-High
5–10	High
10–15	Medium
15–30	Low
≥30	Very-Low

3.3 Influence from strong ground motion

In an earthquake event, fault rupturing and its ground motion will cause severe earthquake disasters, especially for cities with large populations and high buildings. Strong ground motion can cause violent shudders and ground shaking (Anastassiadis and Argyroudis, 2007), which would severely affect the evacuation of residents. In that case, people will change their routes, times, and escape modes of evacuation (Nakanishi, Matsuo, and Black, 2013). Therefore, we analyzed the influence from the predicted strong ground motion data to improve the reliability of the SAA results.

The intensity of earthquakes (e.g., Modified Mercalli intensity scale) is often used to measure the effects of an earthquake at given locations. Here, we converted the predicted PGA data to seismic intensity levels according to the statistical relationship between peak ground acceleration and seismic intensity according to the Chinese national standard China Seismic Intensity Scale (GB_T 17742-2020). The PGA data are those predicted as 10% in the next 50 years (Jia Cheng et al., 2021), based on the inverted geodetic and geological fault slip rates. In the intensity maps both from the geodetic and geological fault slip rates, the urban area of Xichang City is located in the VIII+ intensity zone (Figure 6). According to the China Seismic Intensity Scale (GB_T 17742-2020), most people will be shaken, bumped, and have difficulty walking in intensity VIII areas. When the intensity reaches IX degrees, people walking or running will fall. According to these conditions, we established three sets of impact factors on the accessibility level. Here, we employed different impact factor sets to identify the most suitable set to represent the impacted accessibility distribution in the predicted strong ground motion field (Table 3).

The accessibility level decreases when the time cost for evacuation increases. Hence, we multiplied the time by the inverse of the impact factors (Eq. (1)).

$$T_2 = T_1 \times \frac{1}{I}(1),$$

where T_2 is the time cost for evacuation impacted by strong ground motion, T_1 is the time cost for evacuation based on road network analysis, and I refers to the impact factor on the accessibility level.

After this, we obtained the distribution of time-cost circles under each impact factor set. We employed the impact factor set with
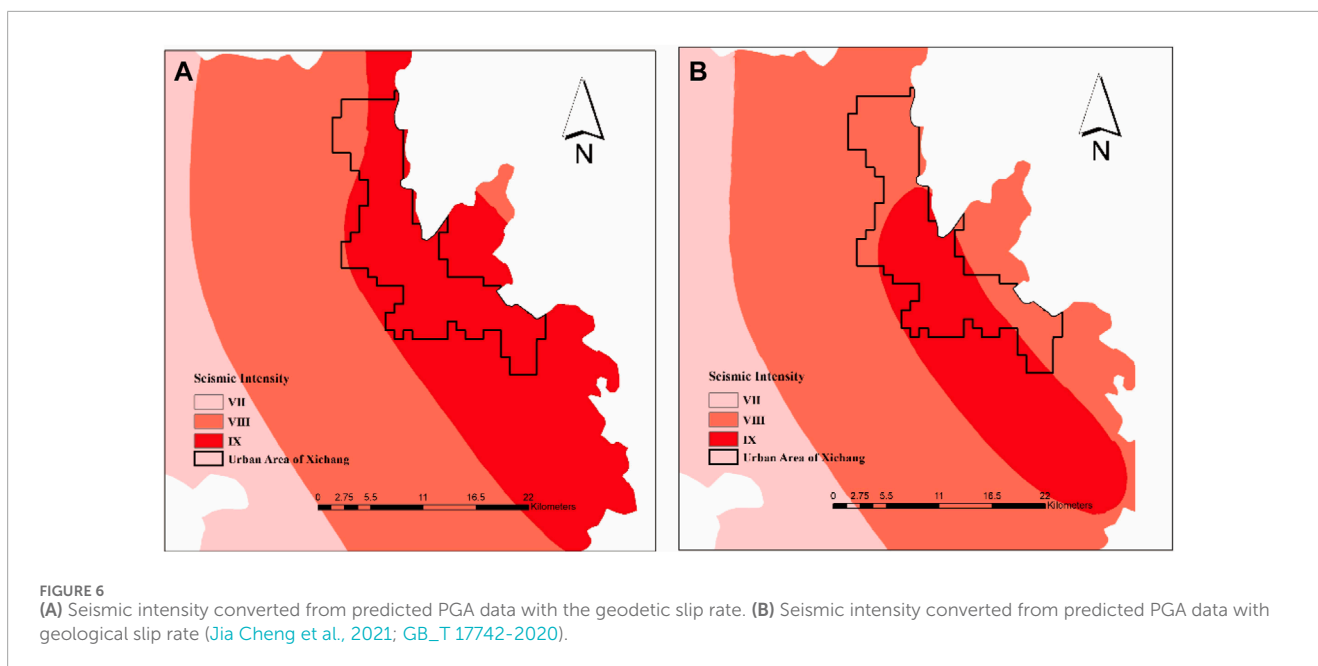
FIGURE 6
(A) Seismic intensity converted from predicted PGA data with the geodetic slip rate. **(B)** Seismic intensity converted from predicted PGA data with geological slip rate (Jia Cheng et al., 2021; GB_T 17742-2020).

TABLE 3 Impact factors on accessibility in different seismic intensity zones.

Seismic intensity degree	Impact factor on accessibility level (I)		
	a	b	c
VIII (8)	0.5	0.6	0.7
IX (9)	0.3	0.4	0.5

clearest demonstration and generated the accessibility level based on the time cost for evacuation (T_2) (Table 2).

3.4 Influence from fault rupturing

Surface rupturing by strong earthquakes can destroy any inhabited structure along the fault lines. On-site investigations and experimental research show that buildings within a rupture zone usually suffer the most severe damage, causing the heaviest disaster (Xu et al., 2016; He et al., 2022). Therefore, we added the effect of surface potential rupturing on the mapped surface lines of the Anninghe fault and the Zemuhe fault from Wu et al. (2023).

The primary setback distance between buildings and the boundary of the active fault rupture zone is set to 15 m (Xu et al., 2016; He et al., 2022). The road surface and the surrounding buildings or structures will probably be damaged within this region, which would significantly impede the evacuation of residents. We generated a buffer zone of linear features with a distance of 15 m around the faults as the setback zone. We set the accessibility level in this region to Very-Low due to the high probability of severe damage.

We then integrated the accessibility level in the setback zone into that affected by the strong ground motion layer, obtaining a comprehensive accessibility distribution map.

4 Results

In this section, we present the result of each procedure (Figure 4).

For data collection, we selected 59 emergency shelter entrances in the urban area of Xichang City (Table 4). Table 4 shows that Xiaomiao Town, Xijiao Town, and Beicheng Block are the top three regarding emergency shelter quantity. Regarding density, emergency shelters are the most densely distributed in Beicheng, Changning, and Changan Blocks. Figure 7A illustrates the spatial distribution of selected emergency shelters and road networks. Our results show that Xichang City has more emergency shelters in the south but fewer in the north (Figure 7A). Emergency shelter distribution is consistent with the spatial distribution of population density. However, on both sides of the Dong River (the area linking Xicheng Block and Dongcheng Block), the number of emergency shelters is not proportional to the large population there. Lizhou and Xisheng Towns, with sparse populations and undeveloped road networks, have no proper emergency shelters according to the remote sensing imagery.

Figure 7B shows the road network-based accessibility distribution map. In this figure, we found that, in areas with dense emergency shelters and well-developed road networks, residents had faster access to emergency shelters (e.g., Beicheng, Xicheng, Dongcheng, and Changning Blocks, eastern Sihe and southern Anning Towns). In rural areas far from emergency shelters, residents have to spend more time accessing emergency shelters (e.g., Lizhou, Xingsheng, northern Anning, Xixiang, Chuanxing, and western Sihe Towns). For example, people living in Xingsheng Town need >20 min to access the nearest shelter, while people in Lizhou and Chuanxing Towns will spend more than 30 min escaping to selected emergency shelters. Figure 9A shows the accessibility level distribution based on road network analysis. In Lizhou, Xingsheng, western Anning, and Chuanxing Towns, the accessibility level is

TABLE 4 Information about selected emergency shelters.

Towns/blocks	Area (km²)	Number of emergency shelters	Emergency shelter density (per km²)	Ranking by quantity	Ranking by density
Xiaomiao Town	45.85	14	0.31	1	7
Xijiao Town	29.25	12	0.41	2	5
Beicheng Block	2.16	7	3.24	3	1
Anning Town	52.64	6	0.11	4	10
Xixiang Town	30.08	4	0.13	5	9
Gaoba Town	22.04	4	0.18	5	8
Xicheng Block	3.92	3	0.77	6	4
Changning Block	1.15	2	1.74	7	2
Changan Block	3.63	2	0.83	7	3
Chuanxing Town	67.17	2	0.03	7	12
Dongcheng Block	2.61	1	0.38	8	6
Sihe Town	80.59	1	0.01	8	13
Xincun Block	14.84	1	0.07	8	11
Xingsheng Town	37.07	0	0	9	14
Lizhou Town	35.32	0	0	9	14

at Very-Low and Low levels, while for towns or blocks with a density of emergency shelters, accessibility presents Very-High and High levels.

After analyzing the impact of strong ground motion based on values of impact factors, we can see that the time cost escaping to emergency shelters increased in general (Supplementary Figure S3). In Figure 7B, we see five grades of classification based on the road network with clear accessibility distribution for different levels. For accessibility levels under the impact of ground motion, some of the time circle distributions are not clearly demonstrated (Figure 8). Figure 8C shows four grades of time-cost circle, while Figures 8A and 8B only display three distinct grades. This phenomenon might be caused by the increasing time cost in an earthquake scenario. Hence, we chose set C for the impact factors to analyze the influences from strong ground motion.

Based on the results in Figure 8C, we generated accessibility level distribution under the effect of strong ground motion. Our results show that the accessibility level in most areas changed after analyzing the influence from the predicted strong ground motion. Figure 9 shows the accessibility level distribution based on different sources. Figure 9A shows different accessibility levels only based on road networks, while Figures 9B and 9C show influence from predicted ground motion data calculated from the geodetic slip rates of the faults and those from geological fieldwork. Figure 9Bs and 9C show the accessibility of Low-level areas diminished to

Very-Low (e.g., southern Lizhou, western Xingsheng, and central Chuanxing Towns). We also noted that the accessibility of Medium- and High-level areas in Figure 9A decreased to Low and Medium levels, as given in Figures 9B and 9C, respectively, such as the area in northeastern, northwestern, and southwestern Anning Town, central Xixiang Town, and the linked area of northeastern Xiaomiao Town, western Xijiao Town, and southwestern Sihe Town. For areas with a Very-High level in Figure 9A, the accessibility level is almost unchanged, such as the areas in Beicheng, Dongcheng, Xicheng, Changning and, Changan Blocks, and northern Gaoba, eastern Xiaomiao, and south-central Anning Towns. In Figures 9B and 9C, the accessibility levels of some specific towns or blocks, such as Anning and Xixiang Towns, cover four levels, including Very-High, Medium, Low, and Very-Low. There are three accessibility levels in Chuanxing Town: Very-High, Medium, and Very-Low. In the towns above, the accessibility level decreases with increasing distance from emergency shelters. While for the Beicheng Block, Dongcheng Block, Xicheng Block, and Changan Block, the accessibility level presents only the type of Very-High level. However, the accessibility level of the entirety of Lizhou Town (within the scope of our study) is only Very-Low.

Considering the fault rupturing effects in an earthquake, we also added the fault surface lines and generated the setback zone of regional mapped active faults. Two large-scale N–S trending faults spread across the urban areas of Xichang City,
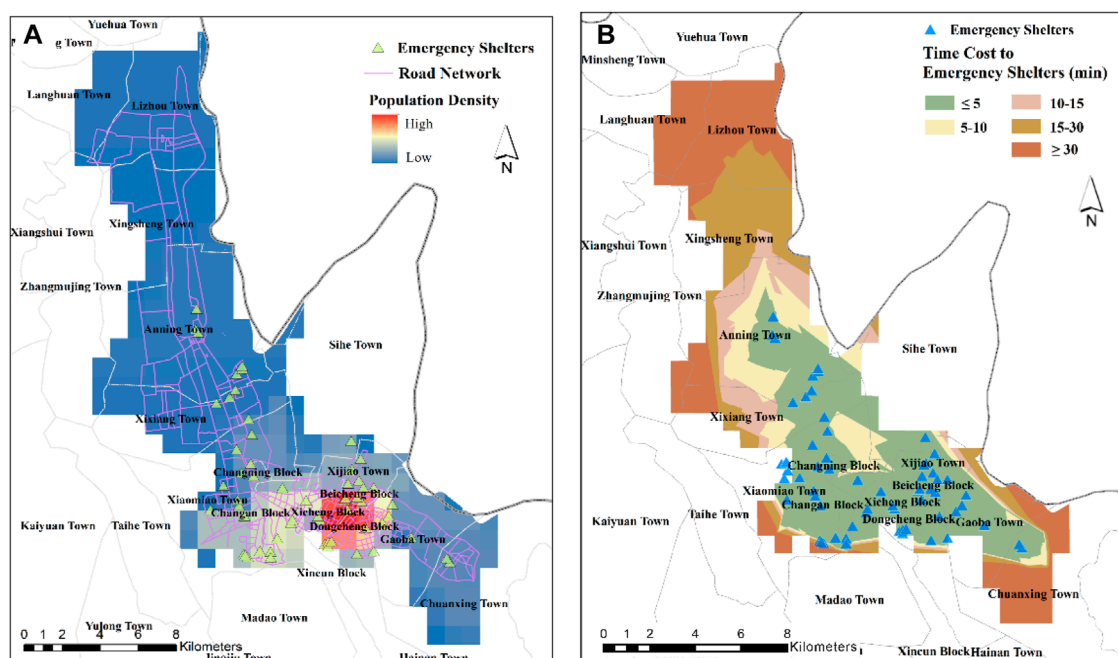
FIGURE 7
(A) Spatial distribution of population density, selected emergency shelters, and simplified road network in the urban area of Xichang City. **(B)** Accessibility to emergency shelters based on road network analysis. We used a network analysis tool, in which the facilities are emergency shelters and the impedance is the time cost for evacuation. Gray lines show the boundary of the towns.

such as Anning, Xixiang, and Xiaomiao Towns (Figure 10). After reassigning the raster value of the setback zone, the accessibility level there is Very-Low. We found the apparent change in the accessibility level in towns or blocks crossed by setback zones, such as the Changan and Xicheng Blocks, at Very-High level decreased to Very-Low.

5 Discussion

In this study, we developed an earthquake scenario-specific framework for SAA. We applied this framework to analyze the practical accessibility of emergency shelters in earthquakes for urban Xichang City. We employed active fault data and predicted strong ground motion data from geodetic and geological slip rates to explore the impact of earthquake damage.
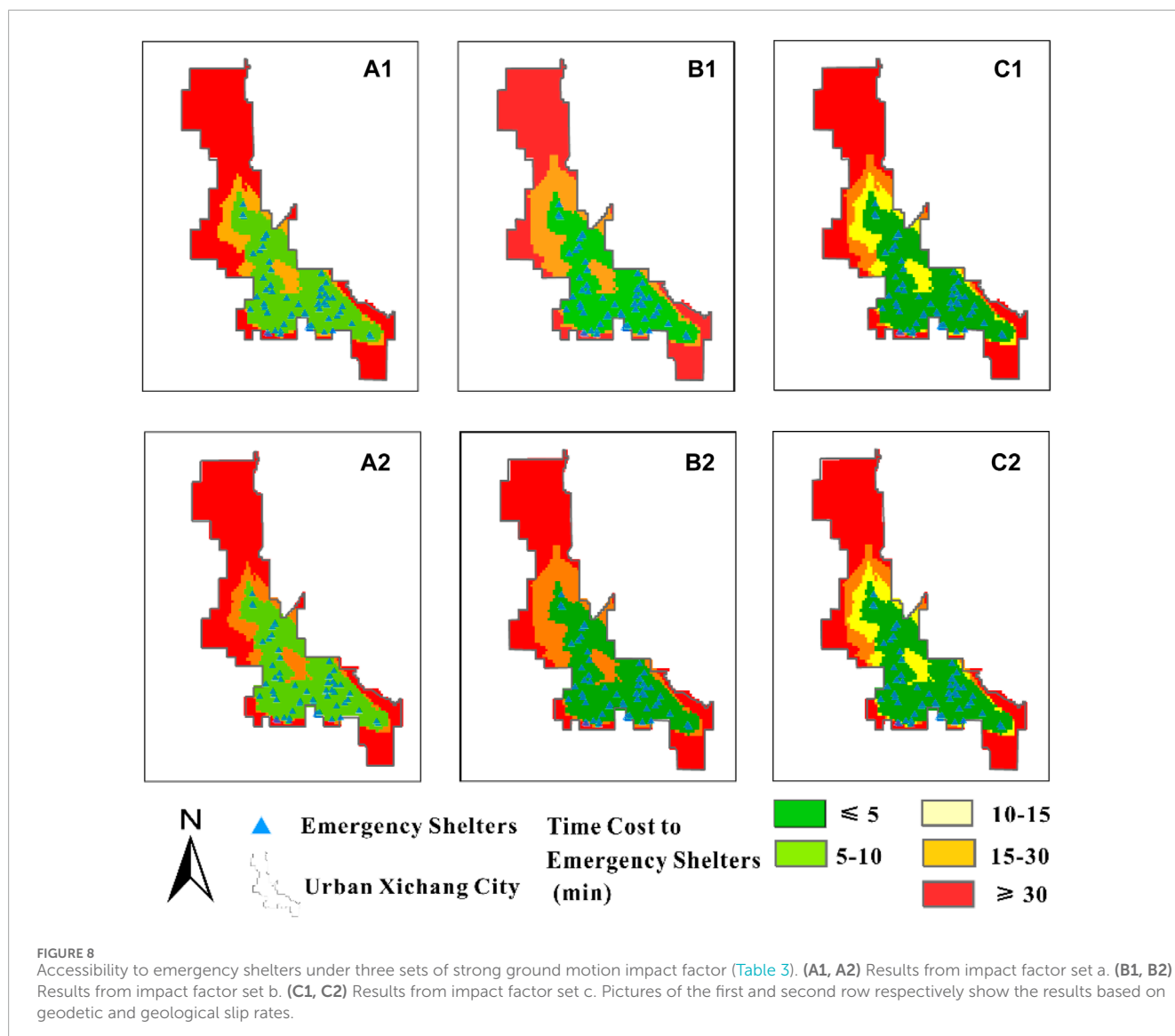
Our results show that the areas with high accessibility to emergency shelters are in the middle of Xichang City, where emergency facilities are densely distributed, such as Beicheng, Dongcheng, Xicheng, Changan and Changning Blocks and Xijiao Town. Low accessibility levels are mainly distributed on the outskirts with few emergency shelters, such as in Lizhou, Xingsheng, central Chuanxing and, and western Anning Towns. Our results show that the spatial variation of accessibility level distribution decreases gradually with increasing distance from emergency shelters. It is worth noting that the accessibility level for Very-High areas almost did not change after adding the effect of potentially strong ground motion (see Figure 9), implying that people living in these areas can escape to emergency shelters in 5 min, even under strong ground

motion from a sudden earthquake. We believed that the dense emergency shelters in urban areas can help residents evacuate in emergencies, even in earthquake scenarios.

Nevertheless, we also found that some areas with few emergency shelters still had a Very-High accessibility level, such as west Dongcheng Block and east Xicheng Block (Figure 11A). These areas have few emergency shelters but large populations and dense residential buildings. Our results show that their accessibility level is Very-High instead of Low. We considered this a result of their well-developed road networks. Thus, a developed road network can improve the accessibility level even in an area with few emergency shelters.

In contrast, an undeveloped road network can diminish accessibility, such as the linked area of northeastern Xiaomiao, western Xijiao, and southwestern Sihe Towns, which have plenty of emergency shelters. Their accessibility level is still Medium rather than Very High. In these areas, the hills (e.g., Panying, Wangjia, Macao, and Majingzi Hills) result in undeveloped road networks (Figure 11B), making evacuation more difficult. Hence, the role of road networks is also crucial to SAA.

We also demonstrated that the impact of potentially strong ground motion and fault rupturing on accessibility to emergency shelters should not be ignored. After analyzing potentially strong ground motion, the accessibility level in most areas declined due to the increasing time cost to access emergency shelters. In areas with mapped faults, the accessibility level decreased as far as Very-Low due to impedance from ruptured surfaces and damaged inhabited structures. These changes in the accessibility level to emergency shelters indicate that SAA should also consider the significant

FIGURE 8
Accessibility to emergency shelters under three sets of strong ground motion impact factor (Table 3). **(A1, A2)** Results from impact factor set a. **(B1, B2)** Results from impact factor set b. **(C1, C2)** Results from impact factor set c. Pictures of the first and second row respectively show the results based on geodetic and geological slip rates.
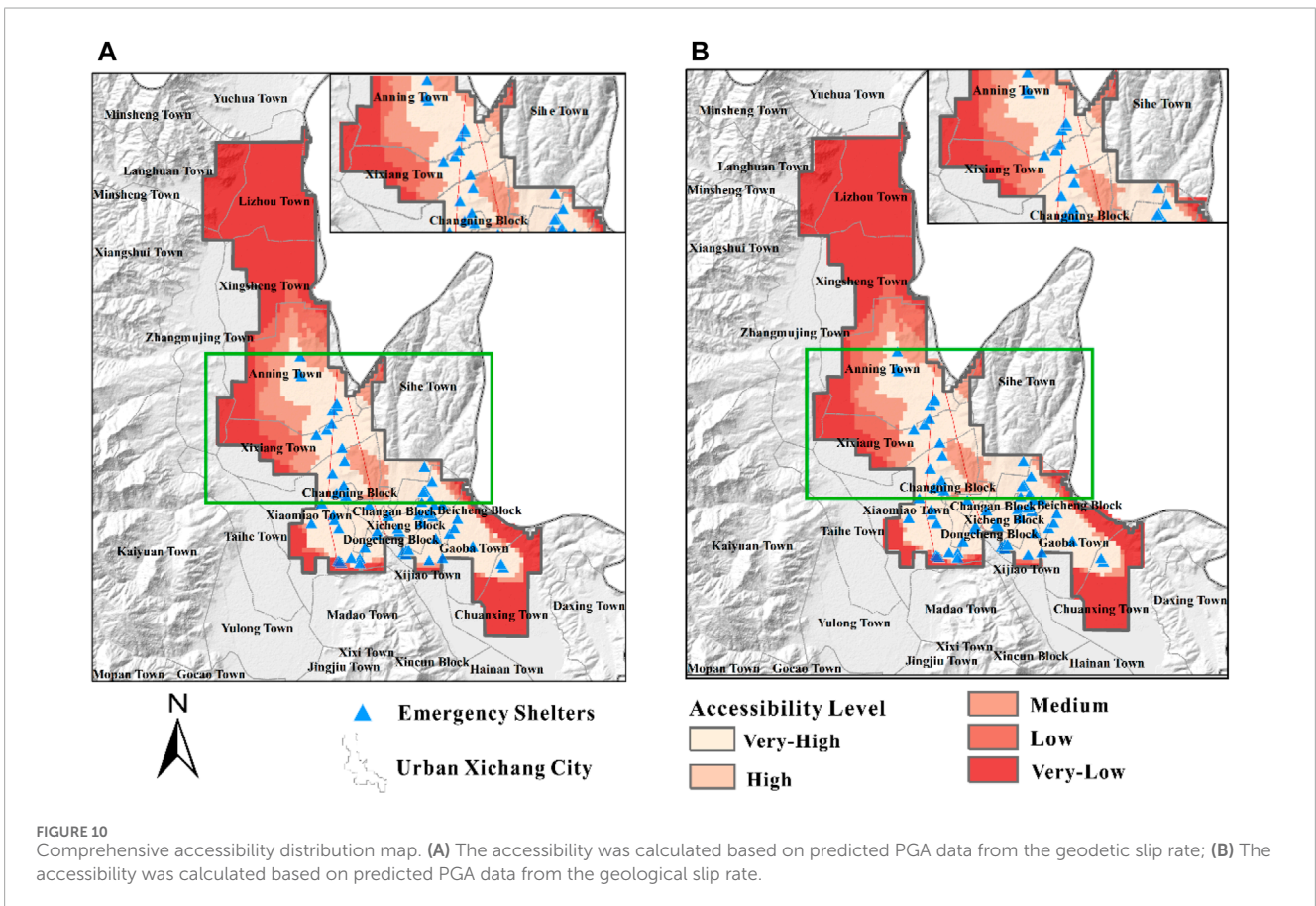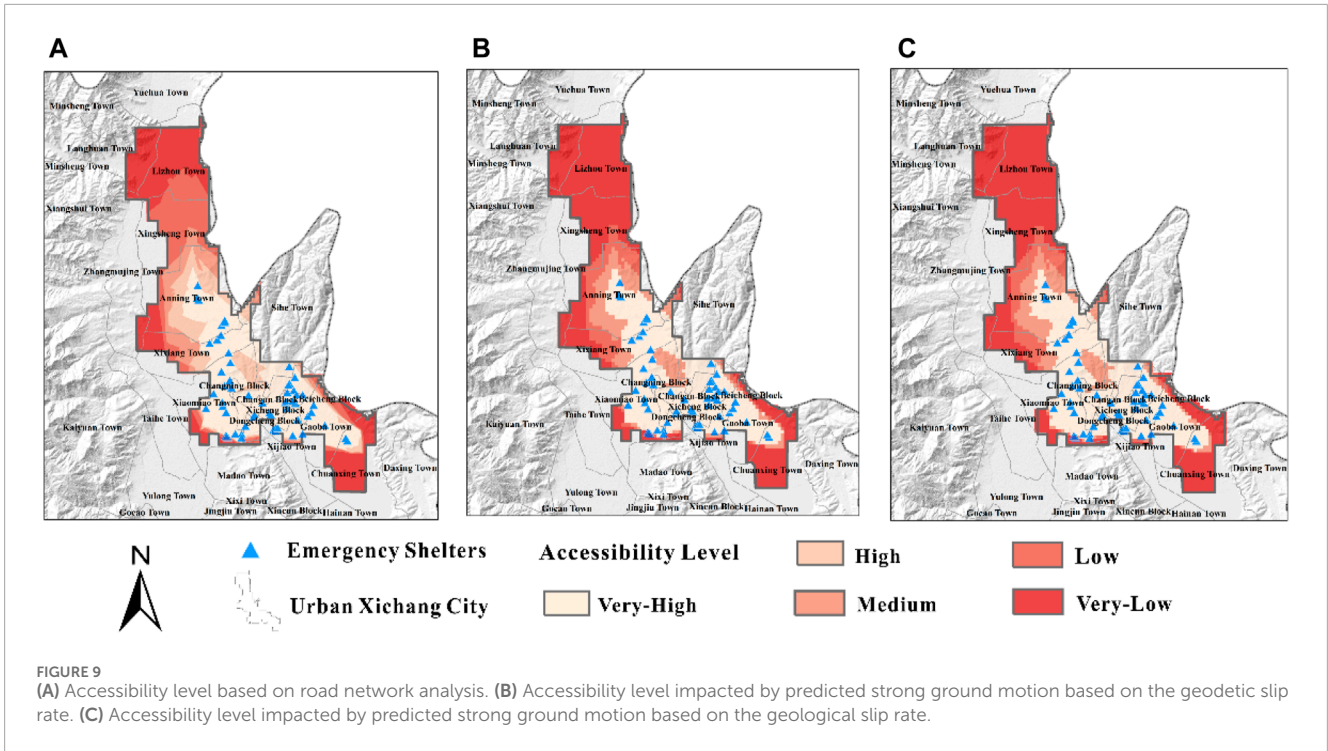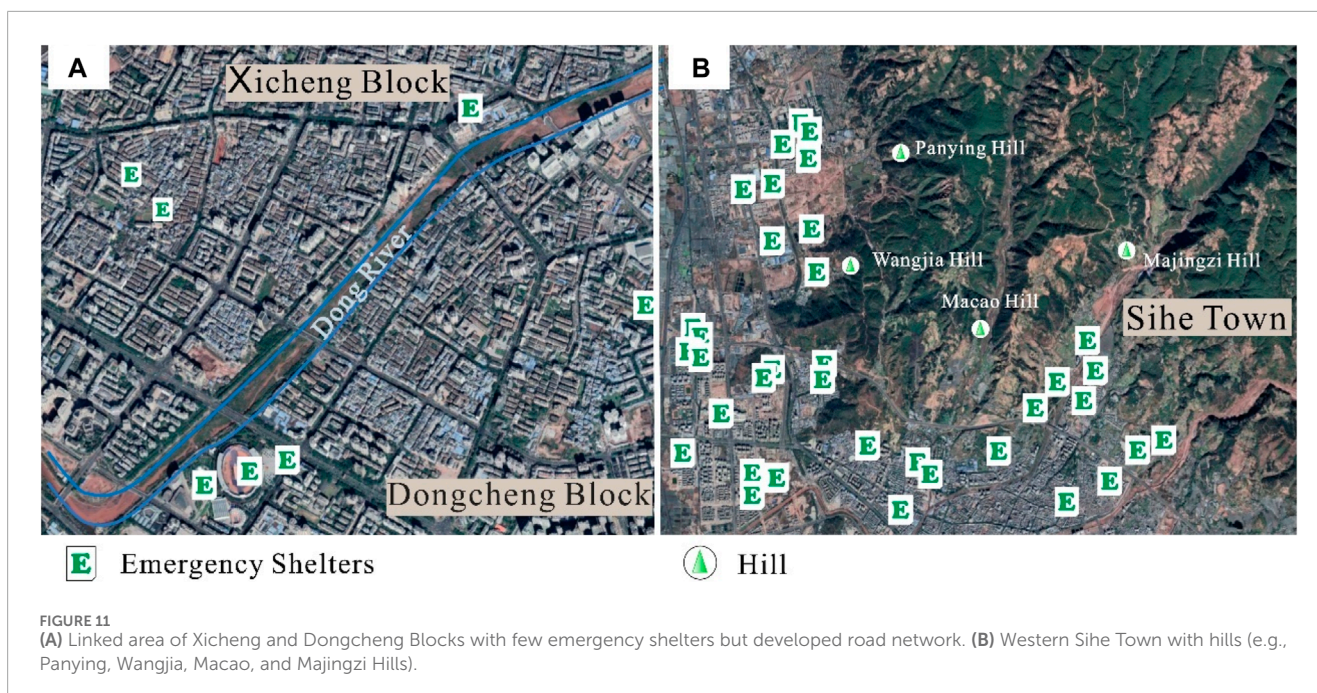
influence of extreme situations, such as strong earthquake scenarios. To cope with such an pessimistic emergency relief situation, the government should take action to refine emergency management. For areas with decreased levels of emergency shelter accessibility, the government should formulate an emergency evacuation plan and guidebook targeted at earthquake scenarios. For towns with multiple accessibility levels, the government should customize emergency evacuation work based on different accessibility levels (e.g., Anning, Xixiang, and Chuanxing Towns).

Our results indicate that people living on urban outskirts have difficulty escaping to emergency shelters. This does not directly mean that residents living there are more vulnerable to an earthquake. For these areas, we only analyzed the spatial accessibility of emergency shelters using the 59 selected emergency shelters, road network data, potential strong ground motion data, and active fault data, but we neglected the role of spaces for shelters, such as farmland and other open fields. In addition, it is easier for residents to exit structures via the lower height of rural residences and in lower populations than urban areas.

In summary, we developed an earthquake scenario-specific framework in the regional SAA for emergency shelters from the following aspects:

1. We developed an earthquake scenario-specific framework to generate a reasonable SAA for emergency shelters. Our framework is reasonable as it integrates the service capacity of urban emergency facilities with earthquake characteristics (strong ground motion and fault rupturing). We also added insights into earthquake scenario characteristics, which contribute to a reasonable simulation of emergency evacuation in earthquakes.

2. We applied this framework in Xichang City. We operated the analysis only in an urban area with an obviously high population density rather than all of Xichang City to obtain more targeted results. We directly labeled the location of entrances instead of the center of emergency shelters to improve the accuracy of accessibility analysis. We referred to the national standard Chinese Seismic Intensity Scale in

FIGURE 9
(A) Accessibility level based on road network analysis. **(B)** Accessibility level impacted by predicted strong ground motion based on the geodetic slip rate. **(C)** Accessibility level impacted by predicted strong ground motion based on the geological slip rate.

FIGURE 10
Comprehensive accessibility distribution map. **(A)** The accessibility was calculated based on predicted PGA data from the geodetic slip rate; **(B)** The accessibility was calculated based on predicted PGA data from the geological slip rate.

FIGURE 11
(A) Linked area of Xicheng and Dongcheng Blocks with few emergency shelters but developed road network. **(B)** Western Sihe Town with hills (e.g., Panying, Wangjia, Macao, and Majingzi Hills).

analyzing the impact of strong ground motion to make the result reliable.

3. Our results can help us understand evacuation to emergency shelters, especially in earthquake scenarios. We identified the practical service area of emergency shelters by analyzing the impact of potentially strong ground motion and fault rupturing. We identified the changes in the accessibility level of emergency shelters in several towns of Xichang City. These results are reasonable because we consider the potential impedance caused by earthquakes in this study.

4. The framework and results of this study can provide a reference for future planning of emergency shelters. Our analysis can assist in the evaluation of seismic vulnerability in terms of casualties and can further support research into the seismic risk of Xichang City.

However, this framework still requires some improvements. 1) We did not consider the relationship between population density and the capacity of emergency shelters. Among the 59 selected emergency shelters, the area varies from 994 m^2 to 2,789 m^2. Considering 2 m^2 per person to avoid overcrowding (Bernardini and Ferreira, 2022), the population capacity of emergency shelters ranges from 497 to 1,394, with a difference of nearly three times as significant.

2) We did not analyze the influence of the performance of buildings. The resistance of buildings can affect emergency evacuations. Building collapse will significantly impede emergency evacuation and even threaten the safety of residents (Guo et al., 2023; Magapu and Setia, 2023). The evacuation performance of buildings (e.g., distribution of separate stairs, maximum density, and vision time) is also related to evacuation efficiency (Chen et al., 2023).

3) In emergency evacuations, various responses to the surrounding environment can lead to multiple ways to avoid

damage. For example, in a tunnel emergency evacuation, people's behavior may be influenced by variables such as the best location to install the board, variable message signs (VMS) contents, and formats and how they interact (Ilkhani et al., 2023).

6 Conclusion

In this study, we proposed an earthquake scenario-specific framework to analyze spatial accessibility to emergency shelters. We applied this framework in urban Xichang City and achieved a comprehensive distribution of accessibility to emergency shelters by adding the impact of strong ground motion and fault rupturing.

Our results show that areas with dense emergency shelters and developed road networks present high accessibility levels (e.g., Beicheng, Dongcheng, and Xicheng Blocks). In contrast, areas far from emergency shelters with undeveloped road networks present low accessibility levels (e.g., Lizhou, Xisheng, Chuanxing, and western Xixiang Towns). As impacted by strong ground motion, the accessibility level decreases in several particular towns (Lizhou, Xingsheng, and Anning). For areas with mapped fault lines, residents and buildings would suffer most damage in earthquakes. The accessibility level to emergency shelters presents a Very-Low level.

Therefore, the SAA of emergency shelters is crucial for efficient evacuation, especially in complex earthquake scenarios. The blocks and towns with few emergency shelters and low accessibility levels must receive greatest attention. The seismic performance of buildings within the setback zone of active faults needs to be emphasized.

Data availability statement

Author contributions

ZW: data curation, formal analysis, software, writing–original draft, and writing–review and editing. JC: funding acquisition, methodology, project administration, supervision, and writing–review and editing. CX: methodology, supervision, and writing–review and editing.

Funding

Conflict of interest

The authors declare that the research was conducted in the absence of any commercial or financial relationships that could be construed as a potential conflict of interest.

The author(s) declared that they were an editorial board member of Frontiers at the time of submission. This had no impact on the peer review process and the final decision.

Publisher's note

All claims expressed in this article are solely those of the authors and do not necessarily represent those of their affiliated organizations, or those of the publisher, the editors, and the reviewers. Any product that may be evaluated in this article, or claim that may be made by its manufacturer, is not guaranteed or endorsed by the publisher.

Supplementary material

The Supplementary Material for this article can be found online at https://www.frontiersin.org/articles/10.3389/feart.2024.1376900/full#supplementary-material

References

Albulescu, A.-C. (2023). Open source data-based solutions for identifying patterns of urban earthquake systemic vulnerability in high-seismicity areas. *Remote Sens.* 15 (5), 1453. doi:10.3390/rs15051453

Amini Hosseini, K., Asadzadeh Tarebari, S., and Mirhakimi, S. A. (2022). A new index-based model for site selection of emergency shelters after an earthquake for Iran. *Int. J. Disaster Risk Reduct.* 77, 103110. July. doi:10.1016/j.ijdrr.2022.103110

Anastassiadis, A. J., and Argyroudis, S. A. (2007). Seismic vulnerability analysis in urban systems and road networks. Application to the city of thessaloniki, Greece. *Int. J. Sustain. Dev. Plan.* 2 (3), 287–301. doi:10.2495/SDP-V2-N3-287-301

Bernardini, G., and Ferreira, T. M. (2022). "Emergency and evacuation management strategies in earthquakes: towards holistic and user-centered methodologies for their design and evaluation," in *Seismic vulnerability assessment of civil engineering structures at multiple scales* (Elsevier), 275–321. doi:10.1016/B978-0-12-824071-7.00002-0

Chang, H.-S., and Liao, C.-H. (2015). Planning emergency shelter locations based on evacuation behavior. *Nat. Hazards* 76 (3), 1551–1571. doi:10.1007/s11069-014-1557-x

Chen, Y., Wang, C., Du, X., Shen, Y., and Hu, B. (2023). An agent-based simulation framework for developing the optimal rescue plan for older adults during the emergency evacuation. *Simul. Model. Pract. Theory* 128, 102797. November. doi:10.1016/j.simpat.2023.102797

Cheng, J., Wu, Z., Liu, J., Jiang, C., Xu, X., Fang, L., et al. (2015). Preliminary report on the 3 august 2014, mw 6.2/ms 6.5 ludian, yunnan-sichuan border, southwest China, earthquake. *Seismol. Res. Lett.* 86 (3), 750–763. doi:10.1785/0220140208

Cheng, J., Xu, C., Ma, J., Xu, X., and Zhu, P. (2023). From active fault segmentation to risks of earthquake Hazards and property and life losses—a case study from the xianshuihe-xiaojiang fault zone. *Sci. China Earth Sci.* 66 (6), 1345–1364. doi:10.1007/s11430-022-1076-y

Cheng, J., Xu, X., Gan, W., Ma, W., Chen, W., and Zhang, Y. (2012). Block model and dynamic implication from the earthquake activities and crustal motion in the southeastern margin of Tibetan plateau. *Chin. J. Geophys* 55 (4), 1198–1212. (in Chinese). doi:10.6038/j.issn.0001-5733.2012.04.016

Cheng, J., Xu, X., Qi, Y., Yang, X., and Chen, H. (2021). Seismic hazard of multi-segment rupturing for the anninghe–zemuhe–daliangshan fault region, southeastern Tibetan plateau: constraints from geological and geodetic slip rates. *Nat. Hazards* 107 (2), 1501–1525. doi:10.1007/s11069-021-04643-7

Elliott, J. R. (2020). Earth observation for the assessment of earthquake hazard, risk and disaster management. *Surv. Geophys.* 41 (6), 1323–1354. doi:10.1007/s10712-020-09606-4

Fang, L., Wu, J., Liu, J., Jia, C., Jiang, C., Han, L., et al. (2015). Preliminary report on the 22 november 2014 M $_w$ 6.1/M $_s$ 6.3 kangding earthquake, western sichuan, China. *Seismol. Res. Lett.* 86 (6), 1603–1613. doi:10.1785/0220150006

Francini, M., Gaudio, S., Palermo, A., and Viapiana, M. F. (2020). A performance-based approach for innovative emergency planning. *Sustain. Cities Soc.* 53, 101906. February. doi:10.1016/j.scs.2019.101906

Gall, M. (2004). Where to go? Strategic modelling of access to emergency shelters in Mozambique. *Disasters* 28 (1), 82–97. doi:10.1111/j.0361-3666.2004.00244.x

General Administration of Quality Supervision, Inspection and Quarantine of the People's Republic of China (2008). GB 21734_2008. *Emergency shelter for earthquake disasters-Site and its facilities (in Chinese)*. Standardization Administration of the People's Republic of China (SAC): Beijing, China.

General Administration of Quality Supervision, Inspection and Quarantine of the People's Republic of China (2020). GB/T 17742-2020. *The Chinese seismic intensity scale (in Chinese)*. Standardization Administration of the People's Republic of China (SAC): Beijing, China.

General Administration of Quality Supervision, Inspection and Quarantine of the People's Republic of China (2017). GBT 33744_2017. *Emergency shelter for earthquake disasters-Guidelines on the operation and management (in Chinese)*. Standardization Administration of the People's Republic of China (SAC): Beijing, China.

General Administration of Quality Supervision, Inspection and Quarantine of the People's Republic of China (2017). GBT 35624_2017. *General technical requirements of urban emergency shelter (in Chinese)*. Standardization Administration of the People's Republic of China (SAC): Beijing, China.

Gui-Xi, Yi, Wen, X.-Ze, and Su, Y.-J. (2008). Study on the potential strong-earthquake risk for the eastern boundary of the sichuan-yunnan active faulted-block, China. *Chin. J. Geophys.* 51 (6), 1151–1158. doi:10.1002/cjg2.1311

Guo, L., Wang, J., Wang, W., and Wang, H. (2023). Performance-based seismic design and vulnerability assessment of concrete frame retrofitted by metallic dampers. *Structures* 57, 105073. November. doi:10.1016/j.istruc.2023.105073

He, X., Xu, C., Xu, X., and Yang, Y. (2022). Advances on the avoidance zone and buffer zone of active faults. *Nat. Hazards Res.* 2 (2), 62–74. doi:10.1016/j.nhres.2022.05.001

Hou, S., and Jiang, H. (2014). An analysis on accessibility of hospitals in Changchun based on urban public transportation. *Geogr. Res.* 33, 915–925. doi:10.11821/dlyj201405010

Huang, Q., Meng, S., He, C., Dou, Y., and Zhang, Q. (2019). Rapid urban land expansion in earthquake-prone areas of China. *Int. J. Disaster Risk Sci.* 10 (1), 43–56. doi:10.1007/s13753-018-0207-4

Iglesias, V., Braswell, A. E., Rossi, M. W., Joseph, M. B., McShane, C., Cattau, M., et al. (2021). Risky development: increasing exposure to natural Hazards in the United States. *Earth's Future* 9 (7), e2020EF001795. doi:10.1029/2020EF001795

Ilkhani, I., Yazdanpanah, M., and Ali, D. (2023). Analysis of drivers' preferences toward content and message format of variable message signs during tunnel emergency evacuation: a case study of niayesh tunnel in tehran. *Int. J. Disaster Risk Reduct.* 93, 103744. July. doi:10.1016/j.ijdrr.2023.103744

Jiang, L., Sang, Q., Jian, W., and Kang, B. (2023). Research on accessibility of park green space in Xicheng district of Beijing based on Gaussian two-step mobile search method. *J. Beijing Univ. Civ. Eng. Archit.* 39, 41–47. (in Chinese). doi:10.19740/j.2096-9872.2023.04.06

Li, W., Sun, J., Zhou, D., and Huang, L. (2023). Dynamics of a diffusion epidemic SIRI system in heterogeneous environment. *South China J. Seismol.* 43 (2), 104–114. (in Chinese). doi:10.1007/s00033-023-02002-z

Liu, C. (1989). Historical materials and preliminary analysis of the 1489 Xichang earthquake. *Sichuan Earthq.* 1, 51–54. (in Chinese).

Liu, X., Wang, p., Guan, L., Lu, H., and Zhang, C. (2017). *GIS spatial analysis*. 3. Beijing, China: Science Press, 89–107. ISBN 978-7-03-051643-5. (in Chinese).

Magapu, S., and Setia, S. (2023). Seismic vulnerability assessment of rc frame structures subjected to seismic excitation: a review. *Mater. Today Proc.* 93, 196–200. July, S2214785323039883. doi:10.1016/j.matpr.2023.07.118

Min, Z., Wu, G., Jiang, Z., Liu, C., and Yang, Y. (2005). *The Catalogue of Chinese historical strong earthquakes (B.C. 2300–A.D. 1911)*. Beijing, China: Seismological Publishing House. (in Chinese).

Nakanishi, H., Matsuo, K., and Black, J. (2013). Transportation planning methodologies for post-disaster recovery in regional communities: the east Japan earthquake and tsunami 2011. *J. Transp. Geogr.* 31, 181–191. July. doi:10.1016/j.jtrangeo.2013.07.005

Qian, H. (2010). Study of environmental assessmental theories and application in city emergency shelters. *Urgent Rescue* 2 (19), 59–63. [in Chinese, with English abstract].

Qin, K. (2010). *Theories and methods of spatial analysis in GIS*. 2. Wuhan, China: Wuhan University Press. ISBN 978-7-307-07576-4. (in Chinese).

Ren, J. (1990). Preliminary study on the recurrence period of strong earthquakes on the fracture zone of Zemuhe, west of sichuan. *Inland Earthq.* 4, 107–115. doi:10.16256/j.issn.1001-8956.1990.02.003

Ren, J., and Li, P. (1993). The characteristics of surface faulting of 1850 earthquake in Xichang, sichuan. *Seismol. Geol.* 15, 97–108. [in Chinese, with English abstract].

Shen, C., Zhou, Z., Lai, S., Lu, Li, Dong, W., Su, M., et al. (2020). Measuring spatial accessibility and within-province disparities in accessibility to county hospitals in shaanxi Province of western China based on web mapping navigation data. *Int. J. Equity Health* 19 (1), 99. doi:10.1186/s12939-020-01217-0

Shen, Z.-K., Jiangning, Lü, Wang, M., and Roland, B. (2005). Contemporary crustal deformation around the southeast borderland of the Tibetan plateau: TIBET SOUTHWEST BORDERLAND DEFORMATION. *J. Geophys. Res. Solid Earth* 110. B11. doi:10.1029/2004JB003421

Su, H., Chen, W., and Cheng, M. (2022a). Using the variable two-step floating catchment area method to measure the potential spatial accessibility of urban emergency shelters. *GeoJournal* 87 (4), 2625–2639. doi:10.1007/s10708-021-10389-3

Su, H., Chen, W., and Zhang, C. (2022b). Evaluating the effectiveness of emergency shelters by applying an age-integrated method. *GeoJournal* 88 (1), 951–969. doi:10.1007/s10708-022-10669-6

Tong, De, Sun, Y., and Xie, M. (2021). Evaluation of green space accessibility based on improved Gaussian two-step floating catchment area method: a case study of Shenzhen City, China. *Prog. Geogr.* 40 (7), 1113–1126. doi:10.18306/dlkxjz.2021.07.004

Wang, Li, Cao, X., Li, T., and Gao, X. (2019). Accessibility comparison and spatial differentiation of xi'an scenic spots with different modes based on Baidu real-time travel. *Chin. Geogr. Sci.* 29 (5), 848–860. doi:10.1007/s11769-019-1073-8

Wen, X. (2000). Character of rupture segmentation of the xianshuihe-anninghe-zemuhe fault zone, western sichuan. *Seismol. Geol.* 22, 239–249. [in Chinese, with English abstract].

Wen, X.-ze, Ma, S.-li, Xu, X.-wei, and Yong-nian, He (2008). Historical pattern and behavior of earthquake ruptures along the eastern boundary of the sichuan-yunnan faulted-block, southwestern China. *Phys. Earth Planet. Interiors* 168 (1–2), 16–36. doi:10.1016/j.pepi.2008.04.013

Wu, X., Xu, X., Yu, G., Ren, J., Yang, X., Chen, G., et al. (2023). China active faults database and its web system. *Prepr. ESSD – Land/Geology Geochem*. doi:10.5194/essd-2023-119

Xu, X., Guo, T., Liu, S., Yu, G., Chen, G., and Wu, X. (2016). Discussion on issues associated with setback distance from active fault. *Seismol. Geol.* 38 (3), 477–502. [in Chinese, with English abstract]. doi:10.3969/j.issn.0253-4967.2016.03.001

Xu, X., Wen, X., Yu, G., Chen, G., Klinger, Y., Hubbard, J., et al. (2009). Coseismic reverse- and oblique-slip surface faulting generated by the 2008 Mw 7.9 wenchuan earthquake, China. *Geology* 37 (6), 515–518. doi:10.1130/G25462A.1

Xu, X., Wen, X., Zheng, R., Ma, W., Song, F., and Yu, G. (2003). Recent patterns of tectonic deformation and dynamics sources of active blocks in the sichuan-yunnan area. *Sci. China* 33, 151–162. (S1) (in Chinese).

Yan, Z. (2023). Analysis of regional traffic accessibility based on ArcGIS. *Stand. Surv. Mapp.* 39, 120–123. doi:10.20007/j.cnki.61-1275/P.2023.02.25

Yi, G., Wen, X., Fan, J., and Wang, S. (2004). Assessing current faulting behaviors and seismic risk of the anninghe-zemuhe fault zone from seismicity parameters. *ACTA Seismol. Sin.* 26, 294–303. [in Chinese, with English abstract].

Zhang, C., Wang, X., and Pei, X. (1998). Strong earthquake in 1536 and newly found surface rupture along Anninghe Fault. *Sichuan Earthq.* 4, 34–50. [in Chinese, with English abstract].

Zhang, P., Deng, Q., Zhang, G., Jin, Ma, Gan, W., Min, W., et al. (2003). Active tectonic blocks and strong earthquakes in the continent of China. *Sci. China Ser. D Earth Sci.* 46, 13–24. S2. doi:10.1360/03dz0002

Zhang, W., and Yun., Y. (2019). Multi-scale accessibility performance of shelters types with diversity layout in coastal port cities: a case study in nagoya city, Japan. *Habitat Int.* 83, 55–64. January. doi:10.1016/j.habitatint.2018.11.002

Zhang, Y. (2020). Research on accessibility of urban parks based on GIS and gravity model: taking the main city of zhengzhou as an example. *Henan Sci.* 38, 733–739. [in Chinese, with English abstract].

Zhao, X., Zheng, Q., Liu, X., and Jin, M. (2018). Study on the planning and allocation of urban park green space based on 2SFCA improved model—a case study of futian district, shenzhen. *Chin. Landsc. Archit.* 34, 95–99. [in Chinese, with English abstract].

Zou, F., Jiang, H., Che, E., Wang, J., and Wu, X. (2023). Quantitative evaluation of emergency shelters in mountainous areas among multiple scenarios: evidence from biancheng, China. *Int. J. Disaster Risk Reduct.* 90, 103665. May. doi:10.1016/j.ijdrr.2023.103665